

A SPITZER IRAC MEASURE OF THE ZODIACAL LIGHT

JESSICA E. KRICK¹, WILLIAM J. GLACCUM¹, SEAN J. CAREY¹, PATRICK J. LOWRANCE¹, JASON
A. SURACE¹, JAMES G. INGALLS¹, JOSEPH L. HORA², WILLIAM T. REACH³
jkrick@caltech.edu

Draft version August 29, 2018

ABSTRACT

The dominant non-instrumental background source for space-based infrared observatories is the zodiacal light. We present *Spitzer* Infrared Array Camera (IRAC) measurements of the zodiacal light at 3.6, 4.5, 5.8, and 8.0 μm , taken as part of the instrument calibrations. We measure the changing surface brightness levels in approximately weekly IRAC observations near the north ecliptic pole (NEP) over the period of roughly 8.5 years. This long time baseline is crucial for measuring the annual sinusoidal variation in the signal levels due to the tilt of the dust disk with respect to the ecliptic, which is the true signal of the zodiacal light. This is compared to both Cosmic Background Explorer Diffuse Infrared Background Experiment (COBE DIRBE) data and a zodiacal light model based thereon. Our data show a few percent discrepancy from the Kelsall et al. (1998) model including a potential warping of the interplanetary dust disk and a previously detected overdensity in the dust cloud directly behind the Earth in its orbit. Accurate knowledge of the zodiacal light is important for both extragalactic and Galactic astronomy including measurements of the cosmic infrared background, absolute measures of extended sources, and comparison to extrasolar interplanetary dust models. IRAC data can be used to further inform and test future zodiacal light models.

Subject headings: cosmology: diffuse radiation — interplanetary medium — infrared: diffuse background

1. INTRODUCTION

The dominant, non-instrumental background source for infrared observations in space is the zodiacal light (ZL), which comes from both scattered and thermal interplanetary dust (IPD) emission. This dust originates mainly from comets and asteroids, as well as a minimal amount from the interstellar medium (Grogan et al. 1996). It has many components, including a smoothly distributed dust cloud along with various clumps and gaps generated by interactions and resonances with the large bodies of the solar system.

Studies of the ZL are applicable to at least three different, unrelated fields of astronomical research. Understanding the ZL allows more accurate studies of the cosmic infrared background (CIB) because it is the dominant error source in those measurements, which has implications for pop III stars. In addition, any absolute measure of extended surface brightness, for example the intracluster light in galaxy clusters, or the outer expanses of nearby galaxies, needs to take into account the contribution from zodiacal light. Lastly, zodiacal models are important in comparison to extrasolar IPD models, especially in using structure in the IPD of stellar systems to find planets.

Measurements of the ZL and models for its properties are based on IRAS (12 - 100 μm) and, primarily, COBE DIRBE (1 - 240 μm) (Boggess et al. 1992; Silverberg et al. 1993). The model most commonly used to date, based on DIRBE data, is Kelsall et al. (1998). The DIRBE data have been subsequently analyzed in conjunction with other data sets to calibrate inconsistencies in various ZL models. Motivated by a desire to measure the CIB, Wright

(1998) and Gorjian et al. (2000) re-derived a ZL model, based on DIRBE data only, making changes to the scattering function and forcing the darkest regions to zero zodiacal emission. Using Infrared Telescope in Space (IRTS) data, Matsumoto et al. (2005) note the need for a correction of order a few percent at near-infrared wavelengths to the Kelsall et al. (1998) model which they attribute to calibration differences between COBE and IRTS, and quoted uncertainties in the model parameters. Pyo et al. (2010) used a hybrid approach to fix most ZL model parameters to be consistent with the Kelsall et al. (1998) model while still allowing their AKARI Infrared Camera data to constrain certain parameters. They find an underestimate by Kelsall et al. (1998) of the earth trailing cloud component and a possible warping of the IPD cloud. We present here an independent evaluation of the ZL model of Kelsall et al. (1998) using *Spitzer* IRAC data (Werner et al. 2004; Fazio et al. 2004).

Spitzer's measurements of the ZL are unique because 1) the spacecraft is not in the same place as the Earth, which gives us new positional information on the IPD cloud and 2) we have a multi-year baseline with approximately weekly cadence. *Spitzer* is in an earth-trailing orbit, slowly drifting behind the earth at a rate of ~ 0.1 AU per year. As of January 2012, *Spitzer* is approximately 1 AU from the earth. We know its position to 500 km, considerably under mission specifications. The weekly cadence allows us to measure the annual variation in the IRAC background levels due to the ZL signal, which in turn will allow for generation of a more accurate model than what could be generated from the ground or a stationary satellite with short duration.

¹ Spitzer Science Center, MS 220-6, California Institute of Technology, Jet Propulsion Laboratory, Pasadena, CA 91125, USA

² Harvard-Smithsonian Ctr. for Astrophysics

³ SOFIA / USRA

The measured surface brightness of the ZL depends on time of year, direction of observation, and location within the dust cloud. The IRAC wavelength range (3.6 - 8 μm) probes regimes of both scattered light and thermal emission; both contribute equally at 3.6, but the longer wavelengths are dominated by thermal emission (Berriman et al. 1994). The DIRBE data show that the zodiacal light typically accounts for just over 50% of the non-instrumental measured sky levels at 3.5 μm , which is about five times the predicted CIB levels. That number jumps to the zodiacal light being 70% of the non-instrumental sky levels at 4.5 μm . At longer wavelengths the sky levels are a few hundred times brighter than the CIB signal. Only redward of $\sim 100 \mu\text{m}$ do other foregrounds become significant (Hauser et al. 1998).

2. OBSERVATIONS & DATA REDUCTION

2.1. *Spitzer* IRAC

As part of the calibration program of IRAC, a field 3.5° from the NEP, with relatively low ZL and no bright stars or extended galaxies is observed with a regular cadence for the purpose of having a shutterless measurement of the bias and dark current in the arrays (Krick et al. 2009). When looking towards the NEP, *Spitzer* observes a near vertical line of sight through the IPD cloud, approximately perpendicular to the dust plane, at a distance of about 1AU from the Sun. During the cryogenic mission from Dec 2003 through May 2009, dark field data were observed twice per campaign, whenever the IRAC instrument was on, which was roughly every two to three weeks. *Spitzer* cryogen was depleted in May 2009, leaving only the 3.6 and 4.5 μm channels functional. From May 2009 through Jan 2010, as the instrument was changing temperature and bias levels, the dark fields flux levels were not comparable to those at a steady temperature, and therefore are not used in this analysis. During the warm mission, from January 2010 to the present, dark fields are observed once per week, with relatively few exceptions.

The data used in this analysis are observed as a set of 18, dithered, 100s Fowler-sampled exposures processed with the calibration pipeline version S18.8(cryo) and S19.0(warm). The longest possible IRAC exposure times were chosen as the best measure of the ZL variations. For the 8 μm data, 50s observations are the longest possible exposure time.

Similar to the basic calibrated data pipeline detailed in the IRAC Handbook ⁴, each of the raw frames was bias subtracted, linearized, flat-fielded, and corrected for various instrumental effects. The bias correction removes the 'first frame' effect which is a dependency of the bias pattern on the time since last readout, or 'delay time'. For the cryogenic mission, a pre-launch library of frames taken at different exposure delay times was interpolated and used as a first frame correction. The warm mission has no such ground data, and therefore no first frame correction. However, we do not expect the lack of a warm first frame correction to effect the ZL measure because it should be a constant offset in the level of the frames since all data was taken with the same delay times in both cryogenic and warm data. After these corrections, a separate program

creates a median image of all the frames (18) within each set of observations using outlier rejection, including a sophisticated spatial filtering stage to reject all stars and galaxies generating a final "skydark" image. The calibration pipeline was designed as the best measure of the dark and bias level in the frames without signal from resolved sources.

Diffuse stray light is a contaminant at the 1% level in both the raw and flat-field images used to correct the pixel to pixel gain effects. We expect this contaminant to be mitigated to less than 0.25% by using 18 dithered frames in the median combine. All data has been converted into physical units of MJy/sr by applying a calibration based on point sources. Because the 5.8 and 8.0 μm detectors suffer from internal scattering caused by photons diffusing around on the chip, the point source calibration is not appropriate for extended sources in these bands. We therefore apply an extended source aperture correction which is a $\sim 30\%$ increase. This correction, which has associated errors, is not critical to the below analysis because it only effects the overall level of the background, and not the annual variation.

To measure the background level in the data, which is composed of ZL, CIB, and any residual instrumental dark current, a gaussian distribution is fitted to the histogram of all pixel values. The mean of that gaussian is considered the true background level for that observation. The mode, as calculated with the technique described in Bickel (2002), is different from the mean by only 0.35%, which is insignificant to our conclusions. Therefore, we use the mean as an adequate representation of the background.

Daily observations of calibration stars throughout the mission show that IRAC photometry in all four channels is stable to 1%, or better, as a function of time. Therefore, it is reasonable to compare photometry over the entire mission without large time-scale systematic drifts.

A completely different calibration product exists to measure the flat fields for IRAC, where observations are taken of high background ecliptic fields. Those observations are not a clean ZL measurement in the same sense as the dark field data because they are taken of a different field every month, and so they do not have the same sampling as the dark field and therefore won't have good enough statistics to compare the sinusoidal variation to the DIRBE data/models.

2.2. COBE DIRBE

We make a direct comparison between IRAC bands 1, 2, 3, & 4 (3.6, 4.5, 5.8, 8.0 μm) and COBE DIRBE bands 3, 4, and 5 (3.5, 4.9, and 12 μm). DIRBE operated in cryogenic mode from November 1989 to September 1990, scanning half the sky every day, building an all-sky map with high coverage and measuring absolute flux using a zero-flux internal calibrator. The DIRBE background has contributions from ZL, astrophysical sources, and CIB. For this analysis we used the calibrated individual observations (CIO), which are the unbinned data for the full cryogenic mission (285 days), with data taken every 1/8 second⁵. DIRBE pixels are roughly 20' on a side. We measured surface brightness in the single pixel that includes the cen-

⁴ <http://irsa.ipac.caltech.edu/data/SPITZER/docs/irac/iracinstrumenthandbook/>

⁵ http://lambda.gsfc.nasa.gov/product/cobe/dirbe_exsup.cfm

ter of the IRAC dark field. At the location of that pixel, over the course of the cryogenic COBE mission, there are roughly 495 individual observations per channel after outlier rejection, where 5% of observations were rejected because they were greater than five sigma from the mean of the distribution. We binned the data to give roughly 34 observations. This binning level was chosen to reduce noise while still retaining the annual ZL signature. Errors are fixed per channel at 3.3%, 2.7% and 5.1% for the three channels respectively (Hauser et al. 1998).

3. RESULTS

Figures 1-4 display the IRAC background levels over the entire 8.5 year lifetime, to date, of *Spitzer*. Cryogenic mission data are shown in green, and warm mission data are shown in blue. The 5.8 and 8 μm channels, shown in Figures 3 and 4, were no longer viable after cryogenic operations ended ~ 5.5 years after launch. Between the cryogenic and warm missions, the detector temperature increased from 15 to 28.7K, consequently increasing the dark current in the images by about 0.6MJY/sr. Therefore, the 3.6 μm surface brightnesses in the cryo and warm data are shown on different scales. The 3.6 μm cryogenic data are much noisier than the 3.6 μm warm data, and all of the 4.5 μm data. The cause of this is uncertain, but could be that the instrument was less stable due to constant power cycling and annealing that only occurred during the cryogenic mission.

The DIRBE data are shown in Figures 1,2,& 4 as solid black points. IRAC 8 μm data are shown with the DIRBE 12 μm channel for comparison. The IRAC 5.8 micron data do not have a good counterpart in the DIRBE filter set. In all cases the DIRBE data is phased in time to fit on top of the IRAC observations even though they were not taken simultaneously. The DIRBE data are also shifted in surface brightness to match the IRAC data. The two data sets do not have the same absolute level because 1) Filter responses are not the same, 2) IRAC data includes an instrumental dark current because IRAC does not have an absolute calibration (see §2.1), and 3) while DIRBE data do have absolute calibration, they include a signal from stars and galaxies that are unresolved in its relatively large beam. Gorjian et al. (2000) measure the contribution of stars to be roughly 10% of the total flux at 3.5 μm .

3.1. Comparison with Zodiacal Light Model

The Kelsall et al. (1998) model is based on DIRBE spectral, temporal and angular information. Briefly, this is a complex, 3D, physical model with over 90 free parameters. It includes contributions from a smooth cloud, three asteroidal debris dust bands, and a circumsolar dust ring near 1AU. Documented sources of uncertainty include non-uniqueness of the model, use of circular, flat orbits when ellipticity and warping are known to exist, and simplistic assumptions about the dust distributions; among others. We emphasize that this is an extremely difficult problem to solve with many components and limited data.

The solid black line in Figures 1-4 shows the predicted ZL level based on Kelsall et al. (1998). The model values have been shifted in surface brightness by 0.02, 0.06, -1.77, and 1.79 MJy/sr in the four channels respectively, to match the IRAC mean cryogenic levels. The bottom

plot of each figure shows the residuals after subtracting the zodiacal light model from the data. The y-axis is shown in units of percent of the surface brightness data.

4. DISCUSSION

The sinusoidal variation in our figures is the ZL signature. We see an annual variation in the ZL contribution to IRAC data because the location of the dark field precesses around the real north ecliptic pole over the course of a year, the dust particle orbits near 1AU are eccentric, and the zodiacal cloud is tilted relative to the Earth's orbital plane (Reach 2010). *Spitzer* is moving above and below the ecliptic dust plane, so that when the telescope is below the plane, it views a larger column density of material towards the NEP, and we see a maximum. Six months later, when the telescope is above the plane, the column towards the NEP is much smaller and we see a minimum ZL signature. Because these data were taken at the NEP, we expect much less ZL than we would observe edgewise through the ecliptic plane.

The absolute surface brightness measured in IRAC data is affected by both astronomical sources (zodiacal, interstellar medium, and extragalactic), and instrumental effects. While DIRBE made an absolute measurement of the instrumental background level, IRAC cannot. Without use of a shutter, IRAC has no direct way of disentangling the dark current and bias level from astronomical sources. We therefore ignore the absolute level in the plots and focus only on the sinusoidal shape as the measurement of ZL variation as a function of time. The IRAC data reduction process (see §2.1) removes all stars and galaxies from the measurement, so the seasonal variation seen is not the result of the resolved star and galaxy content changing. We assume that the ZL is constant over the 25 square arcminute IRAC field of view, and the larger, 1800 square arcminute, DIRBE beam.

Figures 1-4 show significant residuals between the IRAC data and the model, implying inaccuracies in the model. The model curve should fit the IRAC data to higher precision because it has been tailored to the IRAC bands, *Spitzer* orbital position around the sun, and the pointing and time that the data were taken. At 3.6 μm , the cryogenic and DIRBE data are too noisy to glean much information. However the warm mission data show that the model under-predicts the amplitude of the variation by ~ 2 percent. An underestimate of the amplitude could imply either an underestimate of the amount of dust at 1AU, or that the scale height of the dust disk is flatter than modelled leading to *Spitzer* traversing further above and below the concentrated area than predicted.

At 4.5 μm , all IRAC data show a deviation from a sinusoid shape in addition to an underestimate of the amplitude of that sinusoid. The shape change is most clearly evident in the warm mission residuals, which are not sinusoidal in shape. This is the only channel where this shape deviation is seen. A possible explanation for the shape change is that the dust disk is warped (which has been predicted before using IRAS data; Deul & Wolstencroft 1988). The 4.5 μm residuals are larger than the 3.6 μm residuals, which could be giving us color information about the model implying a better knowledge of the dust grain properties. However, it could also be connected to the dif-

ference in the scattered and thermal components of the ZL to the two different wavelength bands, and we have no way of separating those effects. The 4.5 μm residuals also show the overdensity behind the earth as seen previously at 8 μm (see below).

At 5.8 μm , the data are too noisy to be able to glean information from the residuals. Surface brightness values can be negative because a ground-based estimate of the dark current is removed from this data, which is known to differ from the true dark current, of which we have no good measure without use of a shutter. We can rule out large scale changes from the predicted surface brightnesses.

At 8.0 μm , deviations from a simple sinusoidal annual variation over the first year and a half of the mission have been associated with the telescope travelling through an overdensity in dust behind the earth (Reach 2010). This overdensity is seen in Figure 4 where the residuals are mainly negative for the first 1.5 years, and then switch to oscillating around zero. Beyond that overdensity, the residuals look very smooth and constant, implying no further large over- or under-densities at 1AU. In addition to the overdensity, our data show that the model under-predicts the amplitude of the variation by $\sim 5\%$, similar to that seen at 3.6 and 4.5 μm .

5. CONCLUSION

We used IRAC calibration data taken roughly weekly of the NEP to study the ZL component at 3.6, 4.5, 5.8, and 8.0 μm over the course of the currently 8.5 year mission of the instrument. We compare the IRAC data to both COBE DIRBE data and the ZL model of Kelsall et al. (1998) based thereon. COBE DIRBE data are taken from 9.4 months of observations of the same region of the sky as the IRAC data at 3.5, 4.9, and 12 μm . The Kelsall et al. (1998) model is a 90 parameter fit to the DIRBE all sky data at multiple wavelengths from 1-240 μm . All data are shown in Figures 1-4. The sinusoidal variation in the plots is the ZL signature. The Spitzer IRAC data show

a deviation from the Kelsall et al. (1998) model at most at the few percent level. We see an under-prediction of the amplitude of the yearly variation by the model, the presence of an overdensity behind the earth, and possible evidence for a warping in the IPD cloud. These data show both that IRAC can be used for ZL studies and that the ZL model would benefit from the additional information gathered here. A better understanding of the zodiacal light will have broad impacts on studies of the CIB, low surface brightness observations, and extrasolar planets, among other things.

Generating a new ZL model is beyond the scope of this work. It is difficult to know the effect of the few percent discrepancies discussed here on work which uses the Kelsall et al. (1998) model. Because the contribution of the ZL to the background of any given image will change as a function of direction, time of year, and wavelength, there is no easy prescription for the application of these residuals to the conclusions of other papers. It is worth noting that work on the cosmic infrared background is very sensitive to models of the ZL as that type of science is often working at only the few percent level for detections of their signal.

We thank the anonymous referee for useful suggestions on the manuscript. This research has made use of data from the Infrared Processing and Analysis Center/California Institute of Technology, funded by the National Aeronautics and Space Administration and the National Science Foundation. This work was based on observations obtained with the *Spitzer* Space Telescope, which is operated by the Jet Propulsion Laboratory, California Institute of Technology under a contract with NASA. We acknowledge the use of the Legacy Archive for Microwave Background Data Analysis (LAMBDA). Support for LAMBDA is provided by the NASA Office of Space Science.

Facilities: Spitzer (IRAC) COBE (DIRBE)

REFERENCES

- Berriman, G. B., Boggess, N. W., Hauser, M. G., Kelsall, T., Lisse, C. M., Moseley, S. H., Reach, W. T., & Silverberg, R. F. 1994, *ApJ*, 431, L63
- Bickel, D. 2002, *Computational Statistics and Data Analysis*, 39, 153
- Boggess, N. W., Mather, J. C., Weiss, R., Bennett, C. L., Cheng, E. S., Dwek, E., Gulkis, S., Hauser, M. G., Janssen, M. A., Kelsall, T., Meyer, S. S., Moseley, S. H., Murdock, T. L., Shafer, R. A., Silverberg, R. F., Smoot, G. F., Wilkinson, D. T., & Wright, E. L. 1992, *ApJ*, 397, 420
- Deul, E. R. & Wolstencroft, R. D. 1988, *A&A*, 196, 277
- Fazio, G. G., Hora, J. L., Allen, L. E., Ashby, M. L. N., Barmby, P., Deutsch, L. K., Huang, J.-S., Kleiner, S., Marengo, M., Megeath, S. T., Melnick, G. J., Pahre, M. A., Patten, B. M., Polizotti, J., Smith, H. A., Taylor, R. S., Wang, Z., Willner, S. P., Hoffmann, W. F., Pipher, J. L., Forrest, W. J., McMurty, C. W., McCreight, C. R., McKelvey, M. E., McMurray, R. E., Koch, D. G., Moseley, S. H., Arendt, R. G., Mentzell, J. E., Marx, C. T., Losch, P., Mayman, P., Eichhorn, W., Krebs, D., Jhabvala, M., Gezari, D. Y., Fixsen, D. J., Flores, J., Shakoordadeh, K., Jungo, R., Hakun, C., Workman, L., Karpati, G., Kichak, R., Whitley, R., Mann, S., Tollestrup, E. V., Eisenhardt, P., Stern, D., Gorjian, V., Bhattacharya, B., Carey, S., Nelson, B. O., Glaccum, W. J., Lacy, M., Lowrance, P. J., Laine, S., Reach, W. T., Stauffer, J. A., Surace, J. A., Wilson, G., Wright, E. L., Hoffman, A., Domingo, G., & Cohen, M. 2004, *ApJS*, 154, 10
- Gorjian, V., Wright, E. L., & Chary, R. R. 2000, *ApJ*, 536, 550
- Grogan, K., Dermott, S. F., & Gustafson, B. A. S. 1996, *ApJ*, 472, 812
- Hauser, M. G., Arendt, R. G., Kelsall, T., Dwek, E., Odegard, N., Weiland, J. L., Freudenreich, H. T., Reach, W. T., Silverberg, R. F., Moseley, S. H., Pei, Y. C., Lubin, P., Mather, J. C., Shafer, R. A., Smoot, G. F., Weiss, R., Wilkinson, D. T., & Wright, E. L. 1998, *ApJ*, 508, 25
- Kelsall, T., Weiland, J. L., Franz, B. A., Reach, W. T., Arendt, R. G., Dwek, E., Freudenreich, H. T., Hauser, M. G., Moseley, S. H., Odegard, N. P., Silverberg, R. F., & Wright, E. L. 1998, *ApJ*, 508, 44
- Krick, J. E., Surace, J. A., Thompson, D., Ashby, M. L. N., Hora, J., Gorjian, V., Yan, L., Frayer, D. T., Egami, E., & Lacy, M. 2009, *ApJS*, 185, 85
- Matsumoto, T., Matsuura, S., Murakami, H., Tanaka, M., Freund, M., Lim, M., Cohen, M., Kawada, M., & Noda, M. 2005, *ApJ*, 626, 31
- Pyo, J., Ueno, M., Kwon, S. M., Hong, S. S., Ishihara, D., Ishiguro, M., Usui, F., Ootsubo, T., & Mukai, T. 2010, *A&A*, 523, A53
- Reach, W. T. 2010, in *Lunar and Planetary Inst. Technical Report*, Vol. 41, Lunar and Planetary Institute Science Conference Abstracts, 1499+
- Silverberg, R. F., Hauser, M. G., Boggess, N. W., Kelsall, T. J., Moseley, S. H., & Murdock, T. L. 1993, in *Society of Photo-Optical Instrumentation Engineers (SPIE) Conference Series*, Vol. 2019, Society of Photo-Optical Instrumentation Engineers (SPIE) Conference Series, ed. M. S. Scholl, 180-189
- Werner, M. W., Roellig, T. L., Low, F. J., Rieke, G. H., Rieke, M., Hoffmann, W. F., Young, E., Houck, J. R., Brandl, B., Fazio, G. G., Hora, J. L., Gehrz, R. D., Helou, G., Soifer, B. T., Stauffer, J., Keene, J., Eisenhardt, P., Gallagher, D., Gautier, T. N., Irace, W., Lawrence, C. R., Simmons, L., Van Cleve, J. E., Jura, M., Wright, E. L., & Cruikshank, D. P. 2004, *ApJS*, 154, 1
- Wright, E. L. 1998, *ApJ*, 496, 1

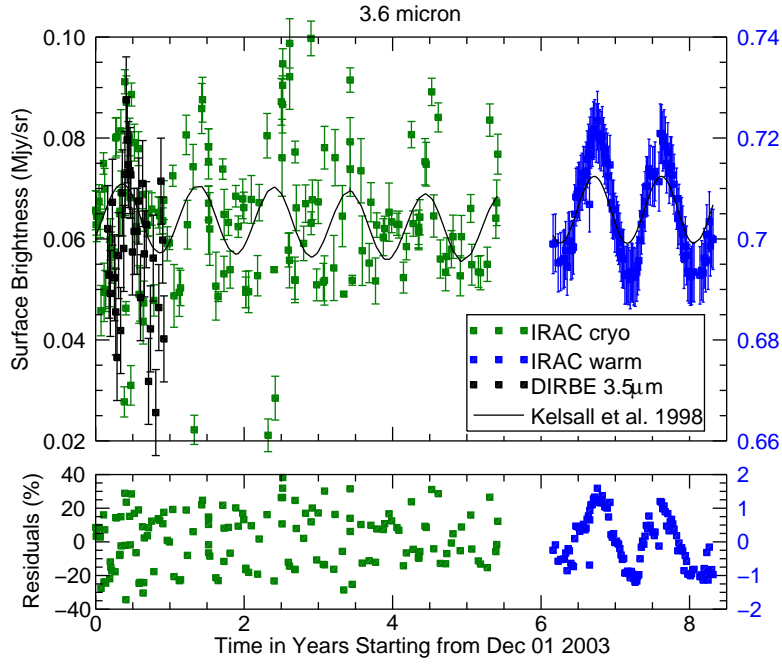


FIG. 1.— **Zodiacal light signature.** Top: IRAC surface brightness at 3.6 μm of the dark field plotted over the timespan in years of the entire Spitzer mission to date. Cryogenic data are shown in green with y-axis labels on the left; warm data are shown in blue with y-axis labels on the right. DIRBE data are overlaid as the black points. The Kelsall et al. (1998) model tailored to the IRAC data is shown as the solid black line. Bottom: Residuals in percent after subtracting the Kelsall et al. (1998) models from the IRAC data. The left y-axis corresponds to the cryogenic residuals and the right y-axis corresponds to the warm residuals. Residual levels range from -20 to 20 kJy/sr for the cryogenic data and -10 to 10 kJy/sr for the warm data.

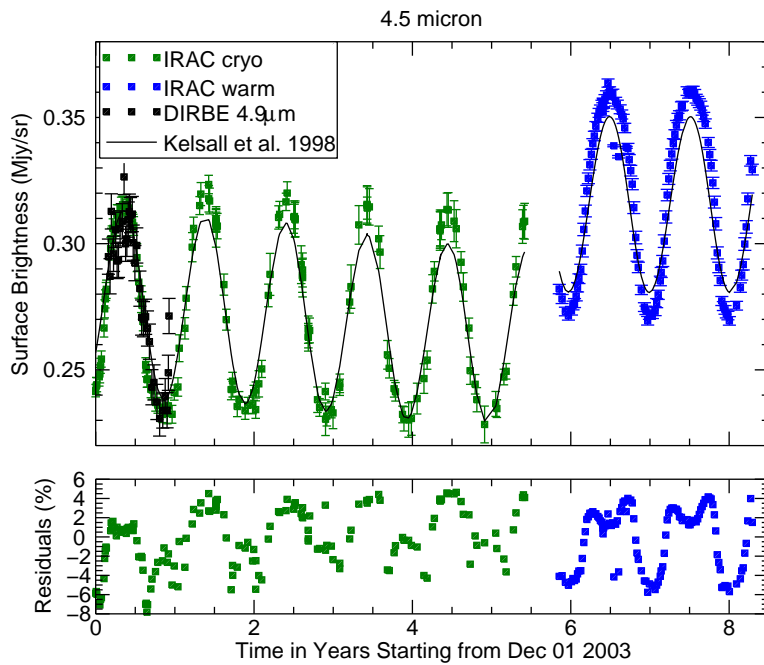


FIG. 2.— Same as Figure 1, but for 4.5 μm (IRAC) and 4.9 μm (DIRBE). Residual levels range from -20 to 15kJy/sr.

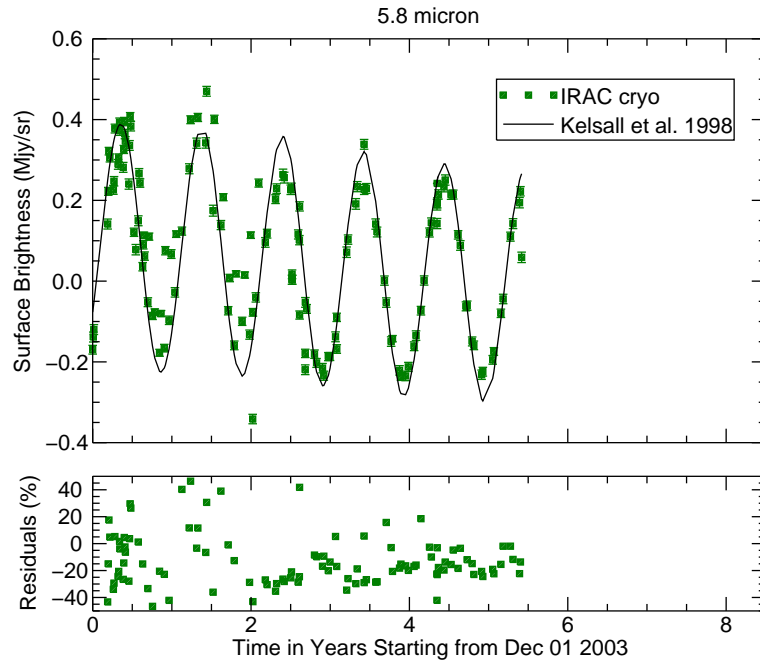


FIG. 3.— Same as Figure 1 for $5.8 \mu\text{m}$ (IRAC). The $5.8 \mu\text{m}$ IRAC channel was only usable during the cryogenic mission. Surface brightness levels can be negative due to lack of an absolute dark current calibration for IRAC (see §2.1. Residual levels range from -100 to 200 kJy/sr .

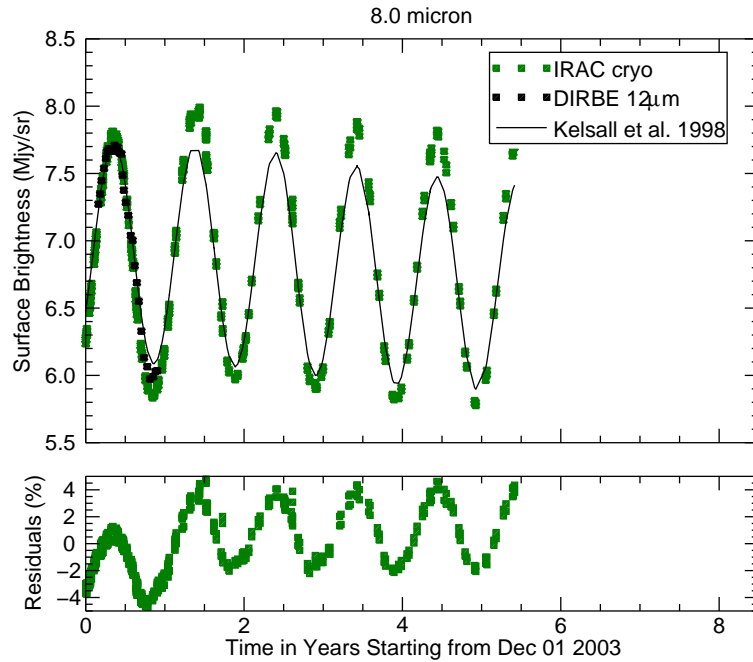


FIG. 4.— Same as Figure 1 for IRAC $8.0 \mu\text{m}$ and DIRBE $12 \mu\text{m}$. The $8.0 \mu\text{m}$ channel was only usable during the cryogenic mission. Residual levels range from -300 to 400 kJy/sr . The negative offset in the residuals for the first 1.5 years is due to the dust overdensity behind the earth.